Local superfluidity in inhomogeneous quantum fluids

Yongkyung Kwon,[1,2] Francesco Paesani,[2,*] and K. Birgitta Whaley[2]
[1]*Department of Physics, Konkuk University, Seoul 143-701, Korea*
[2]*Department of Chemistry and Pitzer Center for Theoretical Chemistry, University of California, Berkeley, California 94720, USA*
(Received 4 January 2006; revised manuscript received 26 September 2006; published 30 November 2006)

A path integral estimator is presented for the local superfluid response at impurities and interfaces in quantum fluids. The estimator is shown to provide a consistent analysis for the rotational response in inhomogeneous Bose systems. Applications are made to the response of superfluid helium in highly structured solvation layers around small linear molecules (CO_2 and OCS) and around a large planar molecule (phthalocyanine) in helium clusters of variable size.

DOI: 10.1103/PhysRevB.74.174522 PACS number(s): 36.40.Ei, 61.46.−w, 67.90.+z

I. INTRODUCTION

Superfluidity is traditionally defined in terms of linear response of a macroscopic system of uniform density.[1] Until recently, the nature of the superfluid fraction in inhomogeneous systems was confined to the recognition that the superfluid density goes to zero near boundaries, e.g., at solid surfaces and at the core of vortex lines. For the bosonic quantum fluids ^{4}He and para-H_2 the associated length scales are less than a nanometer, thus in the regime where interparticle interactions between ^{4}He (or para-H_2) and foreign species are significant. Both adsorption at surfaces[2–7] and solvation of impurities[8] can probe the properties of superfluids at this length scale. The large number of recent experiments on impurity-doped helium droplets[9] have provoked investigation of the meaning and analysis of local superfluidity on a nanometer length scale around a foreign atom or molecule.[10] Analogous studies of molecules solvated by molecular parahydrogen have provided evidence for finite superfluid response, or alternatively of nonclassical rotational inertia,[11] of an inhomogeneous hydrogen cluster at low temperatures.[12–14]

In linear response theory, the global superfluid fraction of a quantum liquid is a tensor quantity defined by the ratio between the quantum moment of inertia I and the classical value I^{cl}. In the principal axis frame, its components are given by

$$f^s|_\alpha = 1 - \frac{I_\alpha}{I_\alpha^{\mathrm{cl}}}, \tag{1}$$

where α denotes a principal axis and the moments of inertia are to be evaluated in the frame of an external field in the limit of zero rotation. A finite value of $f^s|_\alpha$ is also referred to as nonclassical rotational inertia, indicating the reduction of I_α below the classical value I_α^{cl}.[11] Within a discrete path integral representation, the moment of inertia of a quantum liquid can be expressed in terms of the projected area of the Feynman paths[15]

$$I_\alpha = I_\alpha^{\mathrm{cl}} - \frac{4m^2\langle A_\alpha^2\rangle k_B T}{\hbar^2}. \tag{2}$$

Here A_α is the area of a Feynman path projected onto a plane perpendicular to the principal axis $\hat{x}_\alpha$ and the thermal average is taken over the nonrotating bosonic system. When combined with Eq. (1), this gives rise to a path integral estimator for the global superfluid fraction[16]

$$f^s|_\alpha = \frac{4m^2\langle A_\alpha^2\rangle k_B T}{\hbar^2 I_\alpha^{\mathrm{cl}}}. \tag{3}$$

The global fraction f^s represents the superfluid response averaged over all homogeneous and inhomogeneous regions of a finite helium system. This includes interfaces at free surfaces, at solid or liquid boundaries, and at molecular boundaries. Thus the global superfluid fraction is not sensitive to presence of a single impurity molecule. Thus $f_s \sim 0.9(1)$ for pure $(^4\mathrm{He})_{64}$ at $T=0.5$ K,[16] while $f_s \sim 0.83(9)$ for $SF_6(^4\mathrm{He})_{64}$ at $T=0.6$ K.[10] Consequently with this global estimator it is not possible to analyze the anisotropy of superfluid response of a quantum fluid droplet that is induced by a nonsymmetric impurity molecule, except in very small clusters that constitute less than a full solvation shell around the impurity.[13,17] Furthermore, large molecules show multiple solvation layers characterized by a range of densities and local structures. Different extents of superfluidity are to be expected in these layers. Characterization of these differences is a much sought-after goal of helium film studies, but is hard to extract from thermodynamic measurements. One needs instead an analysis for the local superfluidity in different microscopic interfacial or heterogeneous regions that can be accessed by other means. The response to rotation measured by torsional oscillator experiments[18] provides one such route to investigation of the microscopic structure of superfluid response.[3,19–21] For finite helium systems such as free droplets, spectroscopy of embedded impurity molecules can provide an analogous probe of microscopic superfluidity around individual molecules.[8]

The origin of variable local superfluidity around an impurity species may be understood in terms of relative interaction strengths. In the path integral representation,[22] a superfluid is characterized by extended permutation exchange paths throughout the entire helium system, whether this is macroscopic or finite (e.g., nanoscale).[15] A greater interaction of helium with an impurity molecule than with helium itself results in a lowered propensity for permutation exchanges of helium atoms surrounding the molecule, compared to that of helium atoms further away or completely out of range of the molecular interaction. This results in some

helium density close to the molecule being removed from or having reduced participation in the superfluid and a consequent local reduction in the superfluid response.[23] The corresponding local nonsuperfluid response is associated with a nonsuperfluid density whose origin is the molecule-helium interaction. While this nonsuperfluid density is formally a normal helium density, we refer to it as a nonsuperfluid density in order to distinguish it from the usual normal density in bulk helium whose origin is thermal excitations.[24,25] In general, the nonsuperfluid density around a molecule may have both interaction-induced and thermal components.[10,23] In Ref. 23 we introduced an approximate local superfluid estimator that was based on the exchange length of Feynman paths. Using this estimator, local decomposition of superfluid and nonsuperfluid densities in the first solvation shell around the molecule yielded rotational constants of SF_6 and OCS molecules inside the helium droplets that are in good agreement with their experimentally measured values.[10,23] However, this exchange-length-based superfluid estimator was only qualitative and did not provide a rigorous decomposition of the global superfluid response. While long exchange paths often give rise to large projected areas, this is not necessarily so. In addition, the exchange-length-based estimator results in an isotropic superfluid fraction and cannot describe the tensorial nature of the superfluid response. This tensorial nature is critical for understanding the anisotropy in the superfluid environment surrounding a linear molecule as well as close to a heterogeneous interface.

II. LOCAL SUPERFLUID RESPONSE AND LOCAL SUPERFLUID DENSITIES

The notion of superfluidity on a microscopic length scale can be rigorously quantified by making a decomposition of Eq. (3) into local terms, yielding three three-dimensional superfluid response components. Such a decomposition is not unique since local decomposition of a superfluid *fraction* can be made in the context of various different normalizations, representing different physical quantities to which the fraction is applied. Draeger and Ceperley have recently made one such local decomposition that is normalized to the total number of atoms times the global superfluid fraction[26] $N^s|_\alpha = Nf^s|_\alpha$. Here we present an alternative local decomposition of the superfluid fraction that is based on a normalization to the total moment of inertia instead of to the total number of atoms. We show that this decomposition provides an analysis of local superfluidity and a definition of local superfluid density that, unlike both previous local estimators,[23,26] is able to give a consistent analysis of the moment of inertia for a system possessing multiple spatial regions with different local helium/para-H_2 densities. The estimator is thus better suited to microscopic analysis of rotational response of inhomogeneous quantum fluids.

Our local superfluid density is defined by its contribution to the quantum moment of inertia I_α. Within the microscopic two-fluid model,[23] the moment of inertia I_α can be written as

$$I_\alpha = m \int [\rho_{\mathrm{tot}}(\vec{r}) - \rho_s(\vec{r})|_\alpha] r_\perp^2 d^3\vec{r}, \tag{4}$$

where $r_\perp$ is the distance from the principal axis $\hat{x}_\alpha$. Here $\rho_{\mathrm{tot}}(\vec{r})$ and $\rho_s(\vec{r})|_\alpha$ are the total and superfluid number densities of Bose particles, respectively. Since $m\int \rho_{\mathrm{tot}}(\vec{r}) r_\perp^2 d^3\vec{r} = I_\alpha^{cl}$, comparison of Eq. (4) with Eq. (2) gives rise to a definition of the local superfluid response as

$$\rho_s(\vec{r})|_\alpha = \frac{4mk_BT\langle A_\alpha A_\alpha(\vec{r})\rangle}{\hbar^2 r_\perp^2}, \tag{5}$$

where

$$A_\alpha(\vec{r}) = \frac{1}{2}\sum_{i=1}^{N}\sum_{k=1}^{M} (\vec{r}_{i,k} \times \vec{r}_{i,k+1})_\alpha \delta(\vec{r} - \vec{r}_{i,k}). \tag{6}$$

M is the number of time slices in the discrete path integral representation,[15] and $A_\alpha(\vec{r})$ is the sum of all area segments passing through the differential volume $d^3\vec{r}$ and thus represents the local contribution of all paths to the projected area A_α. This superfluid response estimator thus constitutes a local superfluid density that integrates to the correct quantum moment of inertia

$$m\int \rho_s(\vec{r})|_\alpha r_\perp^2 d^3\vec{r} = 4m^2k_BT\frac{\langle A_\alpha^2\rangle}{\hbar^2} = f^s|_\alpha I_\alpha^{\mathrm{cl}}. \tag{7}$$

In addition to a local contribution to the projected area in the numerator, Eq. (5) contains a local factor $r_\perp^2$ in the denominator which describes the local contribution to the classical moment of inertia. The net effect is a local decomposition of the ratio $\langle A_\alpha^2\rangle / I_\alpha^{\mathrm{cl}}$. Incorporating the local nature of the denominator is especially important when the quantum fluid density is strongly inhomogeneous, e.g., helium density around molecules showing multiple solvation shells which possess very different average densities in distinct shells.

We shall refer to Eq. (5) as the *I*-normalized estimator of local superfluid response. This *I*-normalized estimator differs from the local superfluid density that was defined in Ref. 26 by decomposition of the projected area $\langle A_\alpha^2\rangle$ alone:

$$\rho_s^d(\vec{r})|_\alpha = \frac{4m^2Nk_BT\langle A_\alpha A_\alpha(\vec{r})\rangle}{\hbar^2 I_\alpha^{\mathrm{cl}}}. \tag{8}$$

As mentioned above, this decomposition guarantees normalization to $N^s|_\alpha$:

$$\int \rho_s^d(\vec{r})|_\alpha d^3\vec{r} = \frac{4m^2Nk_BT\langle A_\alpha^2\rangle}{\hbar^2 I_\alpha^{\mathrm{cl}}} = N f_s|_\alpha. \tag{9}$$

We shall therefore refer to Eq. (8) as the *N*-normalized estimator. The quantum moment of inertia which results from this local estimator is not consistent with the linear response definition of the moment of inertia (3), since

$$I_\alpha^d = m\int [\rho_{\mathrm{tot}}(\vec{r}) - \rho_s^d(\vec{r})|_\alpha] r_\perp^2 d^3\vec{r}$$

$$= I_\alpha^{\mathrm{cl}} - \frac{4m^2k_BT}{\hbar^2}\int \frac{Nmr_\perp^2}{I_\alpha^{\mathrm{cl}}}\langle A_\alpha A_\alpha(\vec{r})\rangle d^3\vec{r}, \tag{10}$$

which is not equal to Eq. (2). This inconsistency results from the fact that with the definition in Eq. (8), no local decomposition is made of the denominator in Eq. (3). The factor of I_α^{cl}/N in Eq. (8) provides only a global average estimate to the local classical moment of inertia, instead of the true local

contribution $mr_\perp^2$ that is present in the estimator (5). Consequently, a local superfluid density calculated from the N-normalized estimator is expected to be underestimated in regions close to a rotational axis and to be overestimated in regions far from a rotational axis. We shall see in the examples studied below that this is indeed the case and that it can give rise to unphysical behavior of both superfluid fractions and moment of inertia, while the I-normalized estimator provides physically consistent results in all situations. In particular, we will find instances where the N estimator predicts superfluid fractions greater than unity, implying a negative nonsuperfluid fraction. While a negative superfluid fraction is possible in bulk helium in certain situations, the normal fraction is by definition always positive.[25] This unphysical behavior of the N estimator will be seen to imply a negative moment of inertia for an embedded molecule in some cases.

Since superfluidity of a quantum liquid is defined by its response to an external perturbation, here the imposition of rotation, the moment of inertia is a physically measurable quantity relevant to its global manifestation. Therefore, a consistent definition of the local superfluid density should give rise to the correct expression for the quantum moment of inertia. This is the primary motivation for introducing the I-normalized estimator of Eq. (5) for the local superfluid density.

We note that for a homogeneous Bose liquid, the I-normalized superfluid density estimator (5) correctly reduces to a uniform superfluid density distribution, since in this case the distribution of beads $\vec{r}_{i,k}$ in the discrete path integral is uniform on average and the local decomposition of the projected area $A_\alpha(\vec{r})$ in Eq. (6), will then have an $r_\perp^2$ dependence in the limit of small imaginary time step. Substituting Eq. (4) into Eq. (1) shows that a uniform superfluid density for a homogeneous system $\rho_s(\vec{r})|_\alpha \equiv \rho_s|_\alpha$ guarantees that the global superfluid fraction $f^s|_\alpha$ is equal to the ratio of superfluid to total density $\rho_s|_\alpha/\rho_{\rm tot}$. This is the correct behavior and the usual definition of the superfluid fraction for a homogeneous bulk system. In contrast, the N-normalized estimator does not show this behavior in the homogeneous limit, since Eq. (8) does not become uniform in the homogeneous fluid, as a result of the replacement of the local factor $mr_\perp^2$ in the denominator by $I_\alpha^{\rm cl}/N$.

III. LOCAL SUPERFLUID RESPONSE AROUND LINEAR MOLECULES

A. $(^4\mathrm{He})_N$ around CO_2

We first apply the local superfluid response estimator of Eq. (5) to ^{4}He clusters containing a linear CO_2 molecule, i.e., to $CO_2(^4\mathrm{He})_N$. We consider explicitly the response of the helium to rotational motion of the molecule. Since a linear molecule has cylindrical symmetry, the superfluid fraction of the surrounding helium density will have two principal components $f^s|_\parallel$ and $f^s|_\perp$ corresponding to local superfluid densities $\rho_s(\vec{r})|_\parallel$ and $\rho_s(\vec{r})|_\perp$, respectively. The former represents the helium superfluid response to rotations around the molecular axis and the latter the superfluid response to rotations around an axis perpendicular to the molecular axis. Note that with a realistic three-dimensional representation of the molecule, i.e., of the shape and size of its electronic density distribution, both parallel and perpendicular response components can be stimulated by molecular rotation.

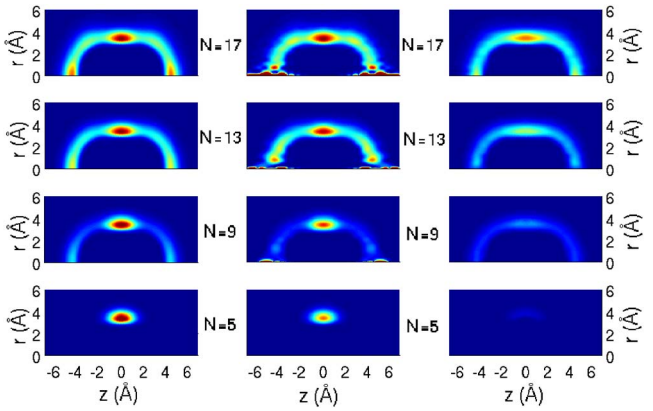

FIG. 1. (Color online) ^{4}He superfluid density distributions for $CO_2(^4\mathrm{He})_N$ clusters computed by the I-normalized estimator of Eq. (5). The CO_2 molecule is located on the z axis with the carbon atom at $z=0.0$ Å, and the two oxygen atoms at $z=\pm 1.1615$ Å, respectively. The coordinate r denotes the distance from the molecular axis (z axis). Left column: total density $\rho(z,r)$, central column: parallel superfluid density $\rho_\parallel^s(z,r)$, right column: perpendicular superfluid density $\rho_\perp^s(z,r)$. All densities in $Å^{-3}$. Color scale goes from blue (0.0 $Å^{-3}$) to red (0.1 $Å^{-3}$).

Figure 1 shows the local ^{4}He superfluid densities $\rho_s(\vec{r})|_\parallel$ and $\rho_s(\vec{r})|_\perp$ around CO_2 obtained with the I-normalized estimator of Eq. (5), together with the total density distribution, for several size ^{4}He clusters corresponding to a single solvation shell ($N=17$) or less ($N=5,9,13$). The corresponding results computed with the N-normalized estimator (8) were previously presented in Fig. 3 of Ref. 17. The large fluctuations in $\rho_s(\vec{r})|_\parallel$ near the molecular axis (z axis) are the effect of the very small value of $r_\perp$ in this region, combined with the small volume of the cylindrical bin used in the computation. With an infinite amount of sampling, in the limit as $r_\perp \to 0$, the superfluid density would be well-behaved since the local contribution to the path areas $A_\parallel(\vec{r})$ also goes to zero as $r_\perp^2$ in this limit [see Eq. (6)].

It is evident from Fig. 1 that for $N=13$ and 17 the parallel superfluid density distributions (central column) closely resemble the corresponding total densities (left column), both in their shape and in their magnitude. This similarity reflects the near unit values of *global* parallel superfluid fraction for these cluster sizes (see Fig. 2 of Ref. 17). In contrast, the parallel superfluid density distributions $\rho_s(\vec{r})|_\parallel$ shown in Fig. 3 of Ref. 17, which were computed with the N-normalized estimator of Eq. (8), are completely different than the total density distributions for all sizes of clusters. Comparison with these earlier calculations shows that the N-normalized estimator significantly underestimates both the local contribution to the parallel superfluidity near the molecular (z) axis, and the perpendicular superfluid density near the x and y axes (i.e., r axis) (compare the right hand columns in Fig. 1 with the corresponding panels in Fig. 3 of Ref. 17). For

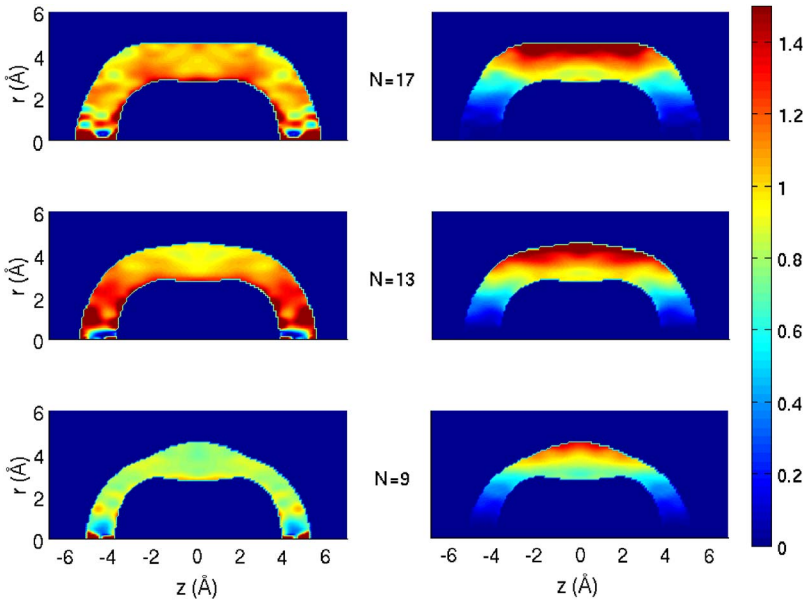

FIG. 2. (Color online) Local distributions of the parallel superfluid fraction $\rho_s(\vec{r})|_{\parallel}/\rho_{\mathrm{tot}}(\vec{r})$ for ^{4}He in $CO_2(^4He)_N$ clusters of three different sizes $N=9,13,17$. Left-hand panels are computed from the I-normalized estimator of Eq. (5), right-hand panels from the N-normalized estimator of Eq. (8). See Fig. 1 for the corresponding total density distributions and definitions of the molecular geometry.

ease of reference, a side-by-side comparison of the local superfluid densities obtained from the two estimators is given as on-line material in Ref. 27. This underestimation of the N-normalized estimator for superfluid density close to the relevant axis of rotation is an example of the overestimation of the local denominator $mr_{\perp}^2$ in Eq. (5) by the global quantity $I_{\alpha}^{\mathrm{cl}}/N$ in the denominator of Eq. (8).

The superfluid density distributions shown in Fig. 1 can be used to further analyze the local behavior of the helium superfluidity by computing the local superfluid fractions around the molecule, which are defined as $\tilde{f}^s(\vec{r})|_{\alpha} = \rho_s(\vec{r})|_{\alpha}/\rho_{\mathrm{tot}}(\vec{r})$, $\alpha=\perp,\parallel$. Figure 2 shows the parallel superfluid fraction distributions in clusters with $N=9,13,17$, and Fig. 3 the corresponding perpendicular superfluid fraction distributions. In both figures the left columns show distributions evaluated from the I-normalized estimator of Eq. (5), while the right columns show the corresponding distributions obtained from the N-normalized estimator of Eq. (8). Figure 2 shows that the local distribution of parallel superfluid fraction computed from the I-normalized estimator is almost uniform within statistical fluctuations, especially for the largest size of cluster considered here, $N=17$, which corresponds to a full solvation shell of helium around CO_2. Such a uniform distribution is expected for a system in which the parallel superfluid density has a very strong similarity with the total density (Fig. 1). Furthermore, for $N=17$ the value of the parallel fraction is approximately unity over the whole solvation shell, consistent with the value for the global parallel fraction.[17] In contrast, the N-normalized estimator results in a very inhomogeneous local parallel superfluid fraction, and furthermore shows unphysical values much larger than unity in some regions (see the dark red region in the right column of Fig. 2). The distributions of perpendicular superfluid fraction in Fig. 3 show similar large differences, with regions of unphysical values in the distribution derived from the

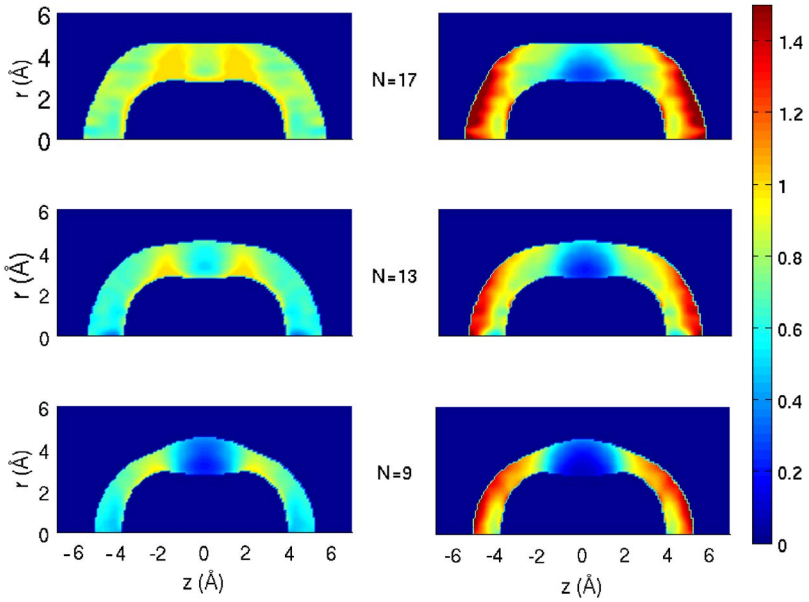

FIG. 3. (Color online) Local distributions of the perpendicular superfluid fraction $\rho_s(\vec{r})|_{\perp}/\rho_{\mathrm{tot}}(\vec{r})$ for ^{4}He in $CO_2(^4He)_N$ clusters of three different sizes $N=9,13,17$. Left hand panels are computed from the I-normalized estimator of Eq. (5), right-hand panels from the N-normalized estimator of Eq. (8). See Fig. 1 for the corresponding total density distributions and definitions of the molecular geometry.

N-normalized estimator and a more homogeneous distribution derived from the *I*-normalized estimator.

The occurrence of regions with fractional superfluidity greater than unity is clearly incorrect behavior for a local estimator of a superfluid fraction. In bulk, the superfluid fraction can be negative, but it is always bounded from above by unity, consistent with a positive semidefinite normal fraction.[25] This overestimation of the superfluid fraction in the regions furthest from the rotational axes is a direct consequence of the underestimation of local contributions to the classical moment of inertia in these regions by the *N*-normalized estimator that was discussed above.

The distributions of local superfluid response around the molecule obtained from the *I*-normalized estimator can be directly related to spectroscopic measurements on the CO_2 molecule in helium clusters.[28,29] The infrared spectroscopic lines correspond to molecular ro-vibrational transitions that are fit to effective rotational Hamiltonians of either rigid rotor or centrifugally distorted rotor form. The complete parallel superfluid response implies zero projection of helium angular momentum on the molecular axis or, equivalently, zero moment of inertia contribution $I_\parallel$ from the helium. In an effective rotational Hamiltonian description, a linear molecule is represented by a rod of zero diameter and thus has no intrinsic parallel moment of inertia. Consequently, in a spectroscopic description, the *K* angular momentum quantum number of the helium solvated molecule is zero and there can therefore be no *Q* branch in the corresponding ro-vibrational spectra.[12,13] This accounts for the lack of a *Q* branch observed in the rovibrational spectra of CO_2 in both small helium clusters[28] and large helium droplets.[29] Evaluating $I_\parallel$ according to Eq. (4) with the *I*-normalized estimator gives zero, consistent with the value obtained from the global parallel superfluid fraction. In contrast, evaluating $I_\parallel$ with the *N*-normalized estimator gives a finite and sometimes unphysical negative value, due to the regions of suppressed or exaggerated local parallel superfluidity predicted by this estimator (Fig. 2). The quantum moment of inertia derived from the *N*-normalized estimator would therefore be completely unreliable and may incorrectly predict some finite *Q*-branch intensity in the molecular rovibrational spectrum.

The different spectroscopic predictions derived from the two perpendicular superfluid response estimators are even more striking. The local suppression of perpendicular superfluidity can result in an increase in the effective moment of inertia of the linear molecule.[13,17] Within linear response, this increase can be calculated quantitatively from rigid coupling of the local nonsuperfluid component $\rho_{ns}(\vec{r}) = \rho_{\mathrm{tot}}(\vec{r}) - \rho_s(\vec{r})|_\perp$ to the molecular rotation, as first proposed in Ref. 23. For heavier molecules, this rigid coupling can be justified within a complete quantum mechanical analysis of the coupled molecule-helium system.[30] For CO_2, the global perpendicular superfluid fraction was used in Ref. 17 to calculate the helium contribution to the moment of inertia and hence the effective rotational constant *B* of the solvated molecule. As discussed there, the two-fluid theory with local nonsuperfluid densities computed by linear response to the molecular rotation is expected to be accurate for CO_2 since the helium distribution is relatively unaffected by the molecular rotation for this molecule.[27] The consistent decomposition of the moment of inertia in the *I*-normalized estimator allows for an accurate estimate of the increase in the CO_2 effective moment of inertia to be calculated from integration over $\rho_{ns}(\vec{r})$ according to Eq. (4). Inspection of Eqs. (4) and (7) shows that this should give rise to the same moment of inertia increment as the one computed in Ref. 17 from the global superfluid fraction.

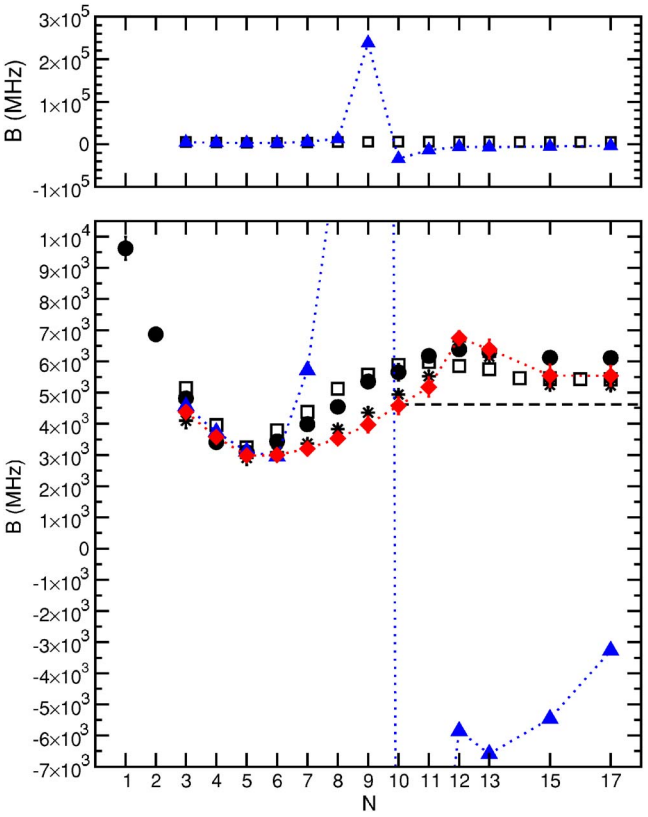

FIG. 4. (Color online) Effective rotational constant *B* for CO_2 in $(^4He)_N$ clusters, obtained from the two-fluid theory using global and local superfluid estimators to calculate the moment of inertia contribution from helium. *B* is shown as a function of cluster size *N* for up to a full solvation shell of helium ($N=1-17$). Red diamonds show values computed from the *I*-normalized estimator of Eq. (5), blue triangles values computed from the *N*-normalized estimator of Eq. (8). Asterisks and filled circles show values computed in Ref. 17 from the global superfluid fraction and with the POITSE method, respectively. Open squares correspond to the experimental values measured in Ref. 28. The dashed line represents the value measured in large helium droplets in Ref. 29.

Figure 4 shows the resulting two-fluid rotation constants derived from both *I*-normalized and *N*-normalized superfluid density estimators and compares these with both the previously calculated values derived from the global perpendicular superfluid fraction and the experimental values of Ref. 28. We see that the *B* values obtained from integration over the *I*-normalized local estimator are extremely close to the previous values calculated from the global superfluid fraction, confirming the consistency of the *I*-normalized estimator for superfluid response to the molecular rotational motion. Furthermore, both of these sets of values are also very close to the experimentally measured values. The small differences between these two calculations visible for *N*

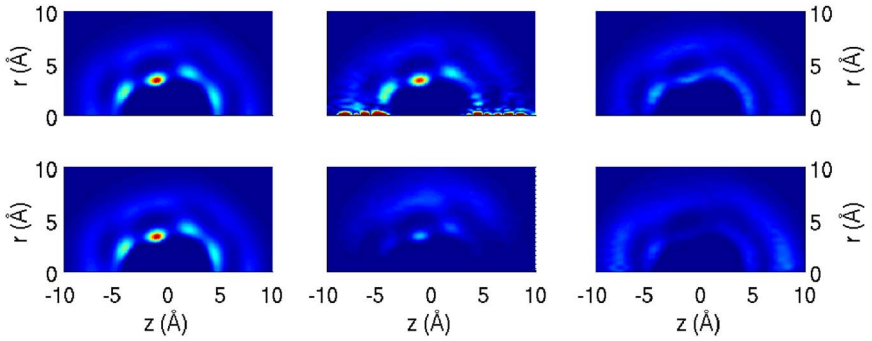

FIG. 5. (Color online) Contour plot of the total density (left column) of $N=64$ ^{4}He atoms around an OCS molecule, together with the parallel (central column) and perpendicular (right column) superfluid densities at $T=0.31$ K. Top row: superfluid density distributions computed with the I-normalized estimator of Eq. (5). Bottom row: corresponding distributions evaluated with the N-normalized estimator of Ref. 26. The molecule center of mass is located at the origin: z is the coordinate along the OCS molecular axis, with the sulfur atom located at $z>0$, and r is the perpendicular radial distance from this axis. Color scale goes from blue (0.0 Å^{-3}) to red (0.2 Å^{-3}).

$=9-11$ shows a small bias in the B values calculated from the local superfluid estimator, which derives from the finite number of grid points used in computation of the total and superfluid density profiles. In contrast, the N-normalized local estimator gives rise to wildly varying values of rotational constant for $N\geqslant 7$. In particular, for $N\geqslant 10$ it produces unphysical negative rotational constants. This results from the gross overestimation of local superfluidity in the regions far from the rotational axis (see dark red region in the right hand column of Fig. 3). Note that the most significant contribution to the moment of inertia comes from regions far from the axis. However, here the local superfluid density computed with the N-normalized estimator is bigger than the total density itself, resulting in an unphysical prediction of negative nonsuperfluid density and a large negative contribution to the effective moment of inertia. The magnitude of this unphysical effect is so large here that the overall rotational constant becomes negative—a totally unacceptable prediction. The only size regime in which the N-normalized estimator gives physically reasonable results is for $N\leqslant 6$, which corresponds to a single ring of helium density around the molecular axis. In this limit the average contribution to the classical moment of inertia I^{cl}/N is approximately the same as its local contribution $mr_{\perp}^2$ and so the N-normalized estimator can easily be seen to give similar results as the I-normalized estimator, explaining the similarity in rotation constants for these very small sizes. Overall, this difference in predicted two-fluid rotational constants and comparison with experimental values reveal the most striking demonstration of the consistency of the I-normalized estimator for local superfluid response around a molecular impurity and of the need for this.

B. $(^4\mathrm{He})_N$ around OCS

As with CO_2, the OCS molecule is linear, but it differs both in being heavier than CO_2 and also in being asymmetric. The OCS$(^4\mathrm{He})_N$ system has been extensively investigated in previous path integral studies,[10,31–33] but the local distribution of superfluid response has not been studied in detail before. We analyze this system here with a larger number of helium atoms, allowing the local superfluid response in a second solvation shell to be studied in addition to that in the first solvation shell.

The top row of Fig. 5 shows the corresponding parallel (central column) and perpendicular local superfluid helium densities (right column) around OCS computed with the I-normalized estimator. It is evident from Fig. 5 that the parallel superfluid density $\rho_s(\vec{r})|_{\parallel}$ shows anisotropic layering structures around OCS that are very similar to those seen in the total helium solvation density distribution (left column), implying that the parallel superfluid response is complete throughout the entire doped cluster. This is confirmed by evaluation of the parallel component of the global superfluid fraction, which is indeed unity within statistical error (see Ref. 32 and discussion below). Just as described for the linear CO_2 molecule above, this complete parallel superfluid response implies zero projection of helium angular momentum on the molecular axis, zero K quantum number of the solvated entity, and therefore no Q branch in the corresponding rotational spectra, accounting for the lack of a Q branch observed in the rotational spectra of OCS inside cold helium droplets.[12,19]

In contrast to this similarity of the parallel superfluid density to the total solvation density, the perpendicular superfluid density $\rho_s(\vec{r})|_{\perp}$ shows a quite different layering structure around the molecule in Fig. 5 (see the top panel in the right column). This is particularly evident in the first solvation shell, where the perpendicular superfluid response is significantly suppressed by the presence of the strongly bound OCS. Approximate estimates for the increase in moment of inertia and reduction of rotational constant within the two-fluid theory have been obtained previously for OCS from the exchange path decomposition isotropic estimate of nonsuperfluid density.[10] While the I-normalized local estimator allows for a more accurate estimate of the increase in molecular effective moment of inertia to be calculated, as we have demonstrated above for CO_2, this becomes more difficult in larger clusters because of the increased statistical fluctuations. An additional concern for an accurate evaluation of the moment of inertia increment for OCS is the effect of the OCS rotational dynamics on the local nonsuperfluid density. Unlike the situation for CO_2, where the local solvation density is not strongly dependent on the molecular rotation, the

OCS rotational dynamics do affect the solvation structure of the surrounding helium liquid[34] and of the superfluid.[33] An accurate estimation of the OCS moment of inertia inside helium droplets requires significantly more extensive sampling of the local helium superfluid density distributions around the molecule as well as an extension of the linear response formalism to allow for the dependence of solvation density on molecular rotation.

The local superfluid density distributions around OCS computed with the *N*-normalized estimator of Eq. (8) are shown in the bottom panels of Fig. 5. It is evident that these distributions show significantly different solvation structures from the corresponding ones in the top panels that are calculated with the *I*-normalized estimator. Similarly to what was seen for CO_2 above, for OCS the *N*-normalized estimator appears to significantly underestimate the local contribution to helium superfluid response near the rotational axes, i.e., near the z axis for the parallel component and near the x and y axes (r axis in Fig. 5) for the perpendicular component. The underestimation here is likewise due to the fact that in the denominator of Eq. (8) the local contribution to the classical moment of inertia close to the axes is unduly weighted by contributions from more distant regions to I_α^{cl}, as discussed in Sec. II.

It is also notable that unlike the behavior of $\rho_s(\vec{r})|_\parallel$ computed with the *I*-normalized estimator, the solvation structure of $\rho_s^d(\vec{r})|_\parallel$ (center panel) bears little similarity to the total density distribution (left panel), especially in the first shell region. Consequently, it is not surprising that integration over the first shell results in a value of parallel fraction considerably less than unity [$f_\parallel^s \sim 0.35$ (Ref. 32)]. This implies finite helium angular momentum projection on the molecular axis and finite intensity of *Q*-branch features in the molecular rotational spectra, in contradiction to experiments.[12,19]

Finally, we note that for both of these linear molecules CO_2 and OCS, the above results show complete parallel superfluid response when this is computed consistently with the *I*-normalized estimator. Thus there is no evidence for a purely thermal reduction in the parallel superfluid response within the first solvation layer, in contrast to what was found for the longer $(HCN)_3$ linear complex with the *N*-normalized estimator $\rho_s^d(\vec{r})$ in Ref. 26. That reduction may be due to the abovementioned fact that the *N*-normalized estimator underestimates the local superfluidity near a rotational axis, as a result of replacing the local contributions to the classical moment of inertia by its global average.

IV. REGIONAL LOCAL SUPERFLUIDITY

We can also evaluate the contributions to superfluid response in larger subregions, e.g., in one of multiple solvation layers around a large molecule, or in a single adsorption layer on a bulk surface. This can be done by defining a locally averaged fraction over a subregion X as in Ref. 35:

$$f_s(X)|_\alpha = 1 - \frac{\Delta I_\alpha}{\Delta I_\alpha^{\mathrm{cl}}} = \frac{4m^2 k_B T}{\hbar^2 \Delta I_\alpha^{\mathrm{cl}}} \int_{V_X} \langle A_\alpha A_\alpha(\vec{r})\rangle d^3\vec{r}. \quad (11)$$

Here V_X is the volume of region X and ΔI^{cl} the contribution to the classical moment of inertia from region X. The analogous subregion estimator obtained from $\rho_s^d(\vec{r})$ is

$$f_s^d(X)|_\alpha = \frac{\int_{V_X} \rho_s^d(\vec{r})|_\alpha d^3\vec{r}}{\int_{V_X} \rho(\vec{r}) d^3\vec{r}}. \quad (12)$$

Note that both of these definitions of regional average superfluid fraction lead to the global superfluid fraction of Eq. (3) when the region X covers the entire system of Bose fluid.

This regional local superfluid estimator is useful for analysis of the strongly modulated helium solvation layers around the linear OCS molecule in larger helium clusters. Regional averages in both first and second solvation shells around OCS in cluster of $N=64$ ^{4}He atoms were reported in Ref. 32. Several critical differences were observed there between the averages defined by the two local estimators. For the average parallel superfluid fraction, the *N*-normalized estimator shows incorrect physical behavior in both solvation shells. The first shell value is considerably less than unity and implies presence of a *Q* branch in the OCS rotational spectrum, in contradiction to experimental observations (see above), while in the second shell it yields a physically incorrect average value of 1.22(9). The averages obtained from the *I*-normalized estimator are instead unity in both first and second solvation shells, so are both well behaved and consistent with experimental absence of *Q*-branch spectral features. These differences are consistent with the detailed distribution of the local densities shown above (Fig. 5). For the average perpendicular superfluid fraction, Ref. 32 showed that the *I*-normalized estimator gives a first shell value of 0.71, which is considerably larger than the value of 0.28 obtained from the *N*-normalized estimator and is quite similar to the (approximate) value of 0.81 that was obtained from the isotropic exchange length estimate in Ref. 10. In the second shell, the value of average perpendicular fraction from the *N*-normalized estimator is again unphysical (1.22), while the corresponding value from the *I*-normalized estimator is unity.

A second situation in which the regional estimator is useful, is for analysis of local superfluid response in different adsorption layers on extended surfaces, or on larger finite substrates where a sampling of the full three-dimensional density is not computationally feasible. One example of such a system is helium solvation around the phthalocyanine molecule.[35] Phthalocyanine is a large planar aromatic molecule with D_{2h} symmetry, containing a total of 58 atoms (C, N, and H) with multiple aromatic rings. Reference 35 showed that the helium density around phthalocyanine in clusters of up to several hundred helium atoms consists of multiple solvation layers possessing very different structures with different average densities. For $N=100$ there are two layers clearly evident on both sides of the molecule, with a third layer providing a capping region at the ends of the molecule. Following Ref. 35, we define here the two layers parallel to the molecular plane on each side of the molecule as regions I and II (containing 40 and 27 helium atoms each), with region I being closest to the molecule, and the capping regions at the ends of the molecule as region III (33 helium atoms). As was found for the OCS(^{4}He)$_{64}$ cluster above in regions close to the rotation axes, we find large fluctuations

TABLE I. Average local superfluid fractions in regions I, II, and III of $N=100$ ^{4}He atoms around phthalocyanine computed using three different local superfluid estimators at temperatures $T=0.3$ and 0.6 K. Results denoted I are obtained with the I-normalized estimator (11), N with the N-normalized estimator (12), and EL with the exchange-length based estimator of Ref. 23. $f^s_{\text{isotropic}}=(2f^s_{x,y}+f^s_z)/3$ is the isotropic average of the superfluid fractions in each region.

		$f^s_{x,y}$		f^s_z		$f^s_{\text{isotropic}}$		
		I	N	I	N	I	N	EL
0.3 K	I	~0	~0	~0	~0	~0	~0	~0
	II	0.33(8)	0.23(4)	0.56(6)	0.16(5)	0.41(5)	0.21(3)	0.43(4)
	III	0.23(5)	0.29(4)	0.22(5)	0.38(7)	0.23(4)	0.32(6)	0.26(4)
0.6 K	I	~0	~0	~0	~0	~0	~0	~0
	II	0.05(4)	0.06(4)	0.41(5)	0.21(5)	0.17(4)	0.11(4)	0.15(3)
	III	0.06(4)	0.07(5)	0.05(4)	0.06(4)	0.06(4)	0.07(4)	0.04(3)

in the projected areas of the permutation paths. Unlike the OCS case there is no cylindrical symmetry to allow increased efficiency of sampling (on a two-dimensional instead of full three-dimensional grid). Consequently it is not feasible within current finite computational restrictions to sample the local superfluid density on a fine three-dimensional grid within each distinct solvation region. Therefore we average over the volume of each of the regions $X=\text{I},\text{II},\text{III}$ to obtain an estimate of the local superfluid fraction in that region according to Eq. (11). For phthalocyanine this averaging is found to yield manageable statistical errors (of the order of 0.01) in the superfluid fractions. The resulting local superfluid fractions for each of the three different solvation regions around the molecule at the two temperatures $T=0.3,0.6$ K are given in Table I.[36]

These results reveal a very strongly anisotropic and position-dependent local superfluidity around this planar aromatic molecule. In region I, which is the region of greatest binding to the molecular substrate, the local superfluidity is essentially zero in all three directions, i.e., both parallel and perpendicular to the molecular plane. Inspection of the exchange moves shows that in fact the helium atoms in this layer rarely participate in any permutation exchange moves, i.e., they are nearly "dead" with respect to exchange, at both temperatures studied here. In region II, where there is less strong binding to the molecule, there is a strong superfluid response along the axis perpendicular to the molecular plane and running through the center of mass of the molecule $f^s_z \sim 0.56$ at $T=0.3$ K and a weaker superfluid response along the in-plane (parallel) axes $f^s_{x,y} \sim 0.33$ at $T=0.3$ K. In region III, where the binding to the molecule is weakest, the superfluid response is nearly isotropic, with $f^s_z \sim 0.22$ and $f^s_{x,y} \sim 0.22$ at $T=0.3$ K.

Each of these regional responses around the planar phthalocyanine molecule is seen to decrease with increasing temperature. The response in region III decreases isotropically, to approximately 25% of the $T=0.3$ K values at $T=0.6$ K. The response in region II shows a strongly anisotropic temperature dependence: at $T=0.6$ K, $f^s_{x,y}$ and f^s_z have decreased to ~15 and ~73 % of their $T=0.3$ K values, respectively. This anisotropic temperature dependence in region II derives from the greater variation of the molecule-helium potential experienced here for motion around the in-plane axes than for motion around the axis perpendicular to the molecular plane. In contrast, in region III the helium response to rotation is less sensitive to the spatial modulation of the molecule-helium potential as well as to the differences in this around the in-plane and the perpendicular axes. Consequently the response in region III is much more isotropic at both temperatures. The temperature dependences seen here thus reflect the different extent to which the in-plane and perpendicular potential anisotropies induce a nonsuperfluid density[23] as well as the dependence of this effective local excitation on temperature. Note that this planar aromatic molecule has a significantly stronger interaction with helium than either of the two linear molecules studied in Sec. III.

For comparison, we also show in Table I the corresponding values of average local superfluid fractions in each of the three regions that are obtained by integrating over the N-normalized estimator according to Eq. (12), as well as the approximate values obtained from integrating over the original isotropic exchange-length based estimator of Ref. 23. We note that in all three regions the isotropic averages of our new tensorial local superfluid fractions of Eq. (11) $(2f^s_{x,y}+f^s_z)/3$ are identical within the statistical errrors to the corresponding values obtained by using the previous exchange-based estimator. This would appear to reflect a sharp distinction between short and long exchange paths for the helium solvation around this molecule, consistent with its strong binding to helium (see Ref. 10 for a discussion of the convergence of the isotropic approximate estimator). On the other hand, we find that the N-normalized estimator significantly underestimates the local superfluidity of region II, particularly the parallel component f^s_z. This underestimation is similar to that seen in the previous section and has the same origin, namely an overestimation of the denominator resulting from use of the total moment of inertia instead of its local contribution within a given region. For phthalocyanine, the classical moment of inertia which appears in the denominator of the N-normalized density (8) has its largest contribution from region III, which is furthest from the z axis. The contribution to the classical moment of inertia from region

III is much larger than the average classical moment of inertia contribution from helium density in region II, since it is further away from the rotation axis. Thus the average value in the denominator is disproportionately weighted to contributions from helium density outside the region under consideration, resulting in a severe underestimation of the superfluid response in region II.

We see with this example of phthalocyanine once again that the lack of consistency with the moment of inertia in the *N*-normalized estimator is reflected in anomalously low values of the local superfluid fraction f_z^s in some regions. This example illustrates very clearly the basic requirement that the superfluid fraction in a given region should be independent of the classical contributions to the moment of inertia deriving from another region of different average density. This analysis of helium solvation layers around a large planar aromatic molecule shows that the regional average of the *I*-normalized estimator can also sensitively distinguish contributions to the helium response to rotation from adsorption layers with different densities and structures. The estimator should therefore be useful for analysis of helium and hydrogen systems inside nanoporous media,[2,37,38] and of torsional oscillator experiments for these systems.[20,39]

V. CONCLUSIONS

We have introduced a path integral estimator for the local anisotropic superfluid density of Bose fluids around impurities. Unlike the previous tensorial local estimator of Ref. 26, the estimator provides a consistent description of the quantum moment of inertia tensor within the microscopic two-fluid model. We designated the estimator as an *I*-normalized estimator, in contrast to the previous *N*-normalized estimator of Ref. 26. The *I*-normalized estimator provides a measure of local superfluid response that is directly related to microscopic torsional oscillator experiments and related spectroscopic measurements on single probe molecules. It provides a local analysis of rotational response of a quantum fluid and hence of superfluidity for strongly heterogeneous helium systems such as adsorbed layers near surfaces and solvation layers around individual molecules. It was also shown to provide a correct reduction to the bulk superfluid fraction in a homogeneous extended system.

Several examples of rotational response around molecular impurities were presented here. These demonstrated the consistency and accuracy of the *I*-normalized estimator in situations where the *N*-normalized estimator gives unphysical results, including predicted values of superfluid density that are greater than the total density. The unphysical results were seen to be due to the fact that the local contribution to the classical moment of inertia is not correctly represented in the *N*-normalized estimator, resulting in underestimation of superfluid fractions near rotational axes and overestimation far from rotational axes.

In the first example, application of the *I*-normalized local superfluid estimator to the helium solvation around the linear CO_2 molecule in small clusters of $CO_2(^4He)_N$ with $N \leqslant 17$ shows that the parallel superfluid density of helium has a similar solvation structure around the molecule as the total number density, which is consistent with a near unit value of the global parallel superfluid fraction. The perpendicular superfluid density is seen to be significantly smaller than the total number density in the immediate vicinity of the molecule, accounting for the smaller value of the global perpendicular superfluid fraction. The local distribution of the perpendicular response provides detailed insight on a microscopic length scale as to the origin of this reduction. For CO_2, it is found to give rise to rotational constants within a local two-fluid theory that are in good agreement with both previous calculations based on the global perpendicular superfluid fraction and with experimental measurements. Similarly, the complete helium parallel superfluidity is consistent with the observed lack of a *Q* branch in the experimental molecular rotation spectrum. In contrast, as a result of the incorrect representation of the local moment of inertia contribution in the *N*-normalized estimator, the physical predictions from both parallel and perpendicular superfluid densities are found to disagree with spectroscopic measurements. Thus the *N*-normalized parallel response is seen to be erroneously suppressed in the first solvation shell, which would predict a finite intensity of *Q*-branch features in the molecular rotation spectra, in contradiction with experimental findings. More seriously, the *N*-normalized perpendicular response shows unphysical regions of superfluid fraction larger than unity. This is seen to result in negative moments of inertia and consequently in unphysical values of effective molecular rotation constants. These unphysical values predicted by the *N*-normalized local superfluid estimator are in striking contrast to the good accuracy of the rotational constants derived from the *I*-normalized estimator, providing strong evidence for the need of a consistent local decomposition of the helium response to impurity rotation.

A second example for helium solvation around the asymmetric and somewhat heavier linear OCS molecule in a larger cluster of $OCS(^4He)_N$ with $N=64$ produces similar results. Thus the parallel superfluid density distribution computed with the *I*-normalized local estimator is again almost identical to the total density, while the perpendicular superfluid response is smaller in the first solvation shell. Similar differences to those found for CO_2 are seen between the *I*-normalized and *N*-normalized estimators for the OCS molecule. Thus, the latter similarly underestimates superfluidity near the rotational axes and consequently incorrectly predicting finite helium angular momentum projection on the molecular axis and *Q*-branch intensity in the molecular rotational spectrum. It is also found to give unphysical values of local superfluid fractions larger than unity in some regions, while the *I*-normalized estimator is well behaved everywhere. No evidence is found for a pure thermal reduction of the parallel superfluid response around either of these two linear molecules with the consistent *I*-normalized estimator.

Despite the difficulty of overcoming statistical sampling noise when computing three-dimensional superfluid densities with these tensorial local superfluid estimators, we were able to reliably compute the spatial distribution of local superfluid fraction around a molecule. For CO_2 with a full solvation shell the distribution of the local parallel superfluid fraction showed a near uniform value approximately equal to unity in most of the first solvation shell when computed from the

I-normalized estimator, while the distribution obtained from the *N*-normalized estimator showed large spatial variations with unphysical values greater than unity in some locations.

A third application of the *I*-normalized estimator was made to the average local superfluidity in different solvation regions around a large planar aromatic molecule, phthalocyanine, which can be viewed as a prototypical molecular nanosubstrate. The regional superfluidity was found to sensitively distinguish three different regions around the molecule. An interesting observation here is the fact that in all three solvation regions around this strongly bound molecular nanosubstrate, the arithmetic average over all three tensorial components of the regional superfluid fraction is very close to the isotropic approximate estimate that is obtained from an exchange path length estimate of local superfluidity. The results from this example of a significantly larger, planar molecule indicate that the *I*-normalized estimator should be useful for analysis not only of solvation around individual molecules as in the applications presented here, but also for a microscopic analysis of the rotational response of helium and hydrogen systems inside nanoscale porous materials as measured in torsional oscillator experiments.

ACKNOWLEDGMENTS

This research was supported by the Korea Research Foundation (Grant No. KRF-2005-015-C00170 to Y.K.), by the National Science Foundation (Grant No. CHE-0107541 to K.B.W.), and by the Miller Institute for Basic Sciences at Berkeley (K.B.W.).

*Present address: Department of Chemistry and Center for Biophysical Modeling and Simulation, University of Utah, Salt Lake City, Utah 84112, USA.

[1] G. Baym, in *Mathematical Methods in Solid State and Superfluid Theory*, edited by R. C. Clark and G. H. Derrick (Oliver and Boyd, Edinburgh, 1969), p. 121.
[2] M. H. W. Chan, A. W. Yanof, and J. D. Reppy, Phys. Rev. Lett. **32**, 1347 (1974).
[3] P. A. Crowell and J. D. Reppy, Phys. Rev. Lett. **70**, 3291 (1993).
[4] L. M. Steele, C. J. Yeager, and D. Finotello, Phys. Rev. Lett. **71**, 3673 (1993).
[5] M. Pierce and E. Manousakis, Phys. Rev. Lett. **81**, 156 (1998).
[6] M. Pierce and E. Manousakis, Phys. Rev. B **63**, 144524 (2001).
[7] S. A. Khairallah and D. M. Ceperley, Phys. Rev. Lett. **95**, 185301 (2005).
[8] J. P. Toennies, A. F. Vilesov, and K. B. Whaley, Phys. Today **54**, 31 (2001).
[9] J. P. Toennies and A. F. Vilesov, Angew. Chem., Int. Ed. **43**, 2622 (2004).
[10] Y. Kwon, P. Huang, M. V. Patel, D. Blume, and K. B. Whaley, J. Chem. Phys. **113**, 6469 (2000).
[11] A. J. Leggett, Phys. Rev. Lett. **25**, 1543 (1970).
[12] S. Grebenev, B. Sartakov, J. P. Toennies, and A. F. Vilesov, Science **289**, 1532 (2000).
[13] Y. Kwon and K. B. Whaley, Phys. Rev. Lett. **89**, 273401 (2002).
[14] F. Paesani, R. E. Zillich, Y. Kwon, and K. B. Whaley, J. Chem. Phys. **122**, 181106 (2005).
[15] D. M. Ceperley, Rev. Mod. Phys. **67**, 279 (1995).
[16] P. Sindzingre, M. L. Klein, and D. M. Ceperley, Phys. Rev. Lett. **63**, 1601 (1989).
[17] F. Paesani, Y. Kwon, and K. B. Whaley, Phys. Rev. Lett. **94**, 153401 (2005).
[18] E. L. Andronikashvili, Zh. Eksp. Teor. Fiz. **16**, 780 (1946).
[19] S. Grebenev, B. Sartakov, J. P. Toennies, and A. Vilesov, Phys. Rev. Lett. **89**, 225301 (2002).
[20] E. Kim and M. H. W. Chan, Nature (London) **427**, 225 (2004).
[21] E. Kim and M. H. W. Chan, Science **305**, 1101501 (2004).
[22] R. P. Feynman, in *Progress in Low Temperature Physics*, edited by C. J. Gorter (Interscience Publishers, New York, 1955), Vol. 1, p. 17.
[23] Y. Kwon and K. B. Whaley, Phys. Rev. Lett. **83**, 4108 (1999).
[24] L. D. Landau, J. Phys. (Moscow) **5**, 71 (1941).
[25] H. W. Jackson, Phys. Rev. B **19**, 2556 (1979).
[26] E. W. Draeger and D. M. Ceperley, Phys. Rev. Lett. **90**, 065301 (2003).
[27] See EPAPS Document No. E-PRBMDO-74-054641 for a comparison of the helium solvation densities around static and rotating CO_2 molecules and for a side-by-side comparision of the local superfluid densities derived from the *I*-normalized and *N*-normalized estimators. For more information on EPAPS, see http://www.aip.org/pubservs/epaps.html.
[28] J. Tang, A. R. W. McKellar, F. Mezzacapo, and S. Moroni, Phys. Rev. Lett. **92**, 145503 (2004).
[29] K. Nauta and R. E. Miller, J. Chem. Phys. **115**, 10254 (2001).
[30] P. Huang, Ph. D. thesis, University of California, Berkeley, 2003.
[31] Y. Kwon and K. B. Whaley, J. Chem. Phys. **115**, 10146 (2001).
[32] Y. Kwon and K. B. Whaley, J. Phys. Chem. Solids **66**, 1516 (2005).
[33] R. E. Zillich, F. Paesani, Y. Kwon, and K. B. Whaley, J. Chem. Phys. **123**, 114301 (2005).
[34] M. V. Patel, A. Viel, F. Paesani, P. Huang, and K. B. Whaley, J. Chem. Phys. **118**, 5011 (2003).
[35] Y. Kwon and K. B. Whaley, J. Low Temp. Phys. **138**, 253 (2005).
[36] Preliminary results for the regional averages from the *I*-normalized estimator at $T=0.3$ K were presented in Ref. 35.
[37] P. A. Crowell, F. W. Van Keuls, and J. D. Reppy, Phys. Rev. Lett. **75**, 1106 (1995).
[38] M. P. Lilly and R. B. Hallock, Phys. Rev. B **64**, 024516 (2001).
[39] Cao Lie-zhao, D. F. Brewer, C. Girit, E. N. Smith, and J. D. Reppy, Phys. Rev. B **33**, 106 (1986).